



# The synthesis and cyclotetramerisation reactions of aryloxy-, arylalkyloxy-substituted pyrazine-2,3-dicarbonitriles and spectroelectrochemical properties of octakis(hexyloxy)-pyrazinoporphyrazine

Rabia Zeynep Uslu Kobak<sup>a</sup>, Egemen Selçuk Öztürk<sup>a</sup>, Atif Koca<sup>b</sup>, Ahmet Gül<sup>a,\*</sup>

<sup>a</sup> Department of Chemistry, Technical University of Istanbul, TR34469 Maslak, Istanbul, Turkey

<sup>b</sup> Department of Chemical Engineering, Marmara University, TR34722 Goztepe, Istanbul, Turkey

## ARTICLE INFO

### Article history:

Received 26 August 2009

Received in revised form

26 November 2009

Accepted 2 December 2009

Available online 22 December 2009

### Keywords:

Diaminomaleonitrile  
Pyrazine dicarbonitrile  
Cyclotetramerisation  
Pyrazinoporphyrazine  
Electrochemistry  
Cobalt

## ABSTRACT

Novel, aryloxy- and arylalkyloxy-substituted pyrazine dicarbonitriles were synthesized from 5,6-dichloropyrazine-2,3-dicarbonitrile and the corresponding phenol/alcohol derivatives. Cyclotetramerisation of these pyrazine derivatives to form metal pyrazinoporphyrazines in the presence of appropriate metal salts in different solvents such as DMF, quinoline, 2-dimethylaminoethanol and n-hexanol, resulted in decomposition products with the exception of the latter solvent which lead to mainly octakis(alkyloxy)pyrazinoporphyrazines. Cyclic voltammetry and differential pulsed voltammetry of the complexes indicated that cobalt pyrazinoporphyrazine displayed both ligand and metal-based redox processes while zinc and copper derivatives exhibited only ligand-based redox processes. The redox processes of the pyrazinoporphyrazines shifted significantly towards positive potentials compared to those of the common phthalocyanines. The novel compounds were characterised using elemental analysis and spectral techniques.

© 2009 Elsevier Ltd. All rights reserved.

## 1. Introduction

Dicyanopyrazine derivatives, which can be considered as condensation products of diaminomaleonitrile with  $\alpha$ -diketones, have been extensively investigated and are important intermediates in fields such as agricultural, food and medicinal chemistry owing to their unique characteristics [1]. Recently, several substituted dicyanopyrazine derivatives have been reported as electroluminescent materials, synthetic reagents for coloring materials and nonlinear optical materials [2]. When compared with phthalonitrile derivatives, the special features of dicyanopyrazine derivatives arise from the presence of two aza functions in the 1,4-positions in the case of the pyrazine ring. Such special features include an intense chromophoric effect, strong fluorescence (even in solid state), high melting point and high solubility in polar solvents. Owing to the strong electron withdrawing ability of the 5,6-dicyanopyrazine moiety, nucleophilic substitution at the 2- and 3-positions takes place using chloro-leaving groups. The dinitrile compound readily reacts with various nucleophiles such as alcohols [3], thiolates [4], primary [5,6] and secondary amines [7]

and enamines to give various substituted pyrazines [8]. Reaction conditions can be altered by using triethylamine with alcoholates, pyridine with thiolates and sodium hydride in dioxane with amines [9]. Thus, dicyanopyrazine derivatives can be used in the design of a variety of functional materials such as tetrapyrrolynes [10].

Tetrapyrrolynes which are formed by cyclotetramerisation of pyrazine-2,3-dicarbonitriles or their derivatives currently receive considerable attention because of their specific optical properties that result from the 18- $\pi$  electron rich aromatic macrocyclic structure, which can host various metal ions in its central cavity [11]. Tetrapyrrolynes can be used in most of the areas where phthalocyanines are applied such as traditional dyes and pigments, for controlling growth of microorganisms, as electrocatalysts for oxygen reduction, materials for electrochromic displays, media for optical recording, as photosensitive materials in photodynamic cancer therapy, as optical filters and anti-copy inks [12–20].

This paper concerns the synthesis of novel aryloxy- and arylalkyloxy-substituted pyrazine dicarbonitriles. Using general methods, cyclotetramerisation reactions were performed on these pyrazine derivatives to form metal pyrazinoporphyrazines in the presence of appropriate metal salts in different solvents such as DMF, quinoline, n-hexanol, 2-dimethylaminoethanol and

\* Corresponding authors. Tel.: +90 212 285 68 27; fax: +90 212 285 63 86.

E-mail address: [ahmetg@itu.edu.tr](mailto:ahmetg@itu.edu.tr) (A. Gül).

n-pentanol. Furthermore, the voltammetric and spectroelectrochemical properties of the hexyloxy tetrapyrazinoporphyrazines were demonstrated.

## 2. Experimental

### 2.1. Equipment and materials

Electronic spectra were recorded on a Scinco SD-1000 double-beam UV–Vis spectrophotometer and IR spectra on a Perkin Elmer Spectrum One FT-IR (ATR sampling accessory) spectrophotometer. Elemental analyses were performed in the Instrumental Analysis Laboratory of the TUBITAK Marmara Research Centre using Carlo Erba 1106.  $^1\text{H}$  NMR spectra were recorded in  $\text{CDCl}_3$  solution using a Bruker 250 MHz NMR spectrometer. Mass spectra were measured on a Bruker Daltonics MicroTOF mass spectrometer. All starting materials were purchased from major suppliers and used without any further purification. Dimethylformamide was dried over 4 Å molecular sieves and 5,6-dichloropyrazine-2,3-dicarbonitrile (**1**) was obtained in a two step synthesis from diaminomaleodinitrile (DAMN) according to procedures described in the literature [4].

### 2.2. Synthesis

#### 2.2.1. General procedure of pyrazine dicarbonitriles (**2–5**)

5,6-dichloropyrazine-2,3-dicarbonitrile **1** (0.2 g, 1 mmol) and the corresponding hydroxyl derivative that is p-nitrophenol for **2** (0.28 g, 2 mmol), p-cresol for **3** (0.2 mL, 2 mmol), 3-(diethylamino)phenol for **4** (0.33 g, 2 mmol), benzyl alcohol for **5** (0.2 mL, 2 mmol) was stirred in 35 mL THF at 65 °C. Reaction in the presence of triethylamine (0.3 mL, 2.2 mmol) as a base required approximately 18 h to achieve the desired pyrazine dicarbonitriles. The reaction mixture was filtered and the filtrate evaporated to dryness. The residue was dissolved in ethanol and then precipitated by addition of water; the yellow precipitate was collected by filtration and washed with cold hexane and diethyl ether. The residue was further recrystallized from acetone/hexane.

**2.2.1.1. 5,6-Bis(4-nitrophenoxy)pyrazine-2,3-dicarbonitrile (2).** The yield of yellow solid was 0.32 g (78.8%). Melting point (m.p): 250–255 °C. IR,  $\nu_{\text{max}}$  ( $\text{cm}^{-1}$ ): 3114–3074 (CH, aromatic), 2240 ( $\text{C}\equiv\text{N}$ ), 1519, 1346, 1231 (Ar–O–Ar), 1154, 851, 748.  $^1\text{H}$  NMR ( $d_6$ -acetone,  $\delta$ ), ppm: 8.50–7.67 (m, 8H, Ar–H). Calculated for  $\text{C}_{18}\text{H}_8\text{N}_6\text{O}_6$ : C 53.47; H 1.99; N 20.79%. Found: C 53.51; H 2.05; N 20.84%.

**2.2.1.2. 5,6-Bis(4-methylphenoxy)pyrazine-2,3-dicarbonitrile (3).** The yield of pale yellow solid was 0.27 g (79%). M.p: 235–242 °C. IR,  $\nu_{\text{max}}$  ( $\text{cm}^{-1}$ ): 3036 (CH, aromatic), 2960–2925 (CH, aliphatic) 2238 ( $\text{C}\equiv\text{N}$ ), 1443, 1262–1238 (Ar–O–Ar), 1154, 1017, 808.  $^1\text{H}$  NMR ( $d_6$ -acetone,  $\delta$ ), ppm: 7.36–7.21 (m, 8H, Ar–H), 2.38 (s, 6H,  $\text{CH}_3$ ). MS(m/z): 341,038 [ $\text{M}^+$ ]. Calculated for  $\text{C}_{20}\text{H}_{14}\text{N}_4\text{O}_2$ : C 70.17; H 4.12; N 16.37%. Found: C 70.35; H 4.26; N 16.16%.

**2.2.1.3. 5,6-Bis[3-(diethylamino)phenoxy]pyrazine-2,3-dicarbonitrile (4).** The yield of pale yellow solid was 0.31 g (67%). M. p: 137–139 °C. IR,  $\nu_{\text{max}}$  ( $\text{cm}^{-1}$ ): 3078 (CH, aromatic), 2974–2934 (CH, aliphatic) 2236 ( $\text{C}\equiv\text{N}$ ), 1613, 1446, 1270–1232 (Ar–O–Ar), 1129, 1021, 760.  $^1\text{H}$  NMR ( $d_6$ -acetone,  $\delta$ ), ppm: 7.30–6.48 (m, 8H, Ar–H), 3.45–3.36 (q, 8H, N– $\text{CH}_2$ ), 1.18–1.08 (t, 12H,  $\text{CH}_3$ ). Calculated for  $\text{C}_{26}\text{H}_{28}\text{N}_6\text{O}_2$ : C 68.40; H 6.18; N 18.41%. Found: C 68.12; H 6.46; N 18.16%.

**2.2.1.4. 5,6-Bis(benzyloxy)pyrazine-2,3-dicarbonitrile (5).** Synthesis and purification were carried out as outlined for the general

procedure of the pyrazine dicarbonitriles except that DMF was used instead of ethanol in the precipitation process. The yield of pale yellow solid was 0.18 g (52.5%). IR,  $\nu_{\text{max}}$  ( $\text{cm}^{-1}$ ): 3036 (CH, aromatic), 2923 (CH, aliphatic), 2238 ( $\text{C}\equiv\text{N}$ ), 1445, 1345, 1146, 1064–1030 (C–O), 748, 692. MS(m/z): 341,874 [ $\text{M}^+$ ].  $^1\text{H}$  NMR ( $\text{CDCl}_3$ ,  $\delta$ ), ppm: 7.45–7.36 (m, 10H, Ar–H), 5.56 (s, 4H, O– $\text{CH}_2$ ). Calculated for  $\text{C}_{20}\text{H}_{14}\text{N}_4\text{O}_2$ : C 70.17; H 4.12; N 16.37%. Found: C 69.97; H 3.94; N 16.08%.

#### 2.2.2. General procedure of octakis(hexyloxy)pyrazinoporphyrazinato metal (II) (**6–8**)

In order to synthesize the metal pyrazinoporphyrazine, a synthesized pyrazine dinitrile (0.3 mmol of **2**, **3**, **4** or **5**) was reacted with the convenient anhydrous metal salt (zinc (II) acetate, cobalt (II) chloride or copper (II) chloride (0.15 mmol)) in the presence of 10  $\mu\text{L}$  DBU and 1.2 mL of n-hexanol at 135 °C for 6 h under nitrogen atmosphere. After cooling, crude product was precipitated by addition of MeOH (3 mL). The precipitate was filtered off, washed with MeOH and acetone. The product was purified by column chromatography on silica gel ( $\text{SiO}_2$ ) using different solvent or solvent mixture as eluent.

**2.2.2.1. Octakis (hexyloxy)pyrazinoporphyrazinato zinc (II) (6).** This compound was synthesized according to the general procedure of octakis- (hexyloxy)pyrazinoporphyrazinato metal (II). The amounts of the reagents used were as follows: 0.1 g of a dinitrile derivative **2** (0.25 mmol), **3** (0.3 mmol), **4** (0.22 mmol) or **5** (0.3 mmol) and anhydrous zinc (II) acetate [(0.023 g, 0.125 mmol), (0.027 g, 0.15 mmol), (0.02 g, 0.11 mmol) or (0.027 g, 0.15 mmol) for **2**, **3**, **4**, **5**; respectively]. The crude title compound isolated from the mixture was then purified on silica gel column using methanol/chloroform 1:100 mobile phase. When **2**, **3**, **4** or **5** was used as the precursor, yield was 0.024 g (27.5%); 0.028 g (26.9%); 0.014 g (18.4%); 0.022 g (21.2%), respectively. IR,  $\nu_{\text{max}}$  ( $\text{cm}^{-1}$ ): 2956–2858 (CH, aliphatic), 1638, 1441, 1120, 1062 (C–O), 983, 739.  $^1\text{H}$  NMR ( $\text{CDCl}_3$ )  $\delta$ : 4.44–4.20 (m, 16H, O– $\text{CH}_2$ ), 2.33–1.23 (br, 64H,  $\text{CH}_2$ ), 1.01 (br, 24H,  $\text{CH}_3$ ). UV–Vis  $\lambda_{\text{max}}$ (nm) (log  $\epsilon$ ) in  $\text{CHCl}_3$ : 361 (5.34), 624 (5.11). Calculated for  $\text{C}_{72}\text{H}_{104}\text{N}_{16}\text{O}_8\text{Zn}$ : C 62.34; H 7.56; N 16.16%. Found: C 62.04; H 7.78; N 15.96%.

**2.2.2.2. Octakis(hexyloxy)pyrazinoporphyrazinato cobalt (II) (7).** This compound was synthesized according to the general procedure employed for octakis (hexyloxy)pyrazinoporphyrazinato metal (II). The amounts of the reagents were employed: 0.1 g of a dinitrile derivative **2** (0.25 mmol) or **3** (0.3 mmol), anhydrous cobalt (II) chloride [(0.016 g, 0.125 mmol) or (0.019 g, 0.15 mmol) for **2** and **3**; respectively]. The crude title compound isolated from the mixture was then purified on silica gel column using first THF/chloroform 1:5 as the mobile phase and then once more with 2/100 methanol/chloroform. When **2** or **3** was used as the ligand, the yield was 0.033 g (38.4%) and 0.037 g (36%), respectively. IR,  $\nu_{\text{max}}$  ( $\text{cm}^{-1}$ ): 2956–2858 (CH, aliphatic), 1640, 1450, 1137, 1073 (C–O), 981, 750. MS: (m/z): 1380.9 [ $\text{M}^+$ ]. UV–Vis  $\lambda_{\text{max}}$ (nm) (log  $\epsilon$ ) in  $\text{CHCl}_3$ : 334 (5.26), 608 (5.09). Calculated for  $\text{C}_{72}\text{H}_{104}\text{N}_{16}\text{O}_8\text{Co}$ : C 62.64; H 7.59; N 16.23%. Found: C 62.98; H 7.87; N 16.55%.

**2.2.2.3. Octakis(hexyloxy)pyrazinoporphyrazinato copper (II) (8).** This compound was synthesized according to the general procedure used for octakis (hexyloxy)pyrazinoporphyrazinato metal (II). The amounts of the reagents were used as follows: 0.1 g of a dinitrile derivative **2** (0.25 mmol) or **3** (0.3 mmol), anhydrous copper (II) chloride [(0.017 g, 0.125 mmol) or (0.02 g, 0.15 mmol) for **2** and **3**; respectively]. The title compound isolated from the mixture was then purified on silica gel column using methanol/chloroform 2:100 as the mobile phase. When **2** or **3** was used as ligand, yield

was 0.04 g (46.51%) and 0.054 g (52.43%), respectively. IR,  $\nu_{\max}$  ( $\text{cm}^{-1}$ ): 2955–2858 (CH, aliphatic), 1638, 1446, 1133, 1067 (C–O), 982, 745. UV–Vis  $\lambda_{\max}$  (nm) ( $\log \epsilon$ ) in  $\text{CHCl}_3$ : 345 (5.38), 621 (5.48). MS: ( $m/z$ ): 1384.83 [ $\text{M}^+$ ]. Calculated for  $\text{C}_{72}\text{H}_{104}\text{N}_{16}\text{O}_8\text{Cu}$ : C 62.43; H 7.57; N 16.18%. Found: C 62.17; H 7.23; N 15.93%.

### 2.3. Electrochemical analysis

Cyclic voltammetry (CV), differential pulse voltammetry (DPV), and double potential step coulometry (DPSC) measurements were carried out with Gamry Reference 600 potentiostat/galvanostat controlled by an external PC and utilizing a three-electrode configuration at 25 °C. The working electrode was a Pt disc with a surface area of 0.071  $\text{cm}^2$ . The surface of the working electrode was polished with a diamond suspension before each run. A Pt wire served as the counter electrode. Saturated calomel electrode (SCE) was employed as the reference electrode and separated from the bulk of the solution by a double bridge. Ferrocene was used as an internal reference.

Electrochemical experiments were performed in dry dichloromethane (DCM) containing 0.1 mol  $\text{dm}^{-3}$  electrochemical grade tetrabutylammoniumperchlorate (TBAP) as a supporting electrolyte. The solutions were bubbled with high purity  $\text{N}_2$  to remove dissolved  $\text{O}_2$  at least 15 min prior to each run and an  $\text{N}_2$  atmosphere was maintained above the solution during the measurements. For each measurement the reference electrode tip was moved as close as possible to the working electrode so that uncompensated resistance of the solution was a smaller fraction of the total resistance, and therefore the potential control error was low. Moreover, IR compensation was applied to the CV scans to further minimise the potential control error.

The spectroelectrochemical measurements were carried out with an Ocean-optics QE65000 diode array spectrophotometer equipped with the potentiostat/galvanostat utilizing a three-electrode configuration of thin-layer quartz spectroelectrochemical cell at 25 °C. The working electrode was light penetrating Pt tulle. Pt wire counter electrode separated by a glass bridge and an SCE reference electrode separated from the bulk of the solution by a double bridge were used.

## 3. Result and discussion

### 3.1. Synthesis and characterization

5,6-dichloropyrazine-2,3-dicarbonitrile **1**, which is also available commercially [21], was derived from diaminomaleodinitrile DAMN and oxalyl chloride in a two step synthesis according to procedures described in the literature [4]. Compound **1** was treated with *p*-nitrophenol, *p*-cresol and 3-(diethylamino)phenol as phenol derivatives and benzyl alcohol as an arylalcohol in THF at 65 °C. Reaction in the presence of triethylamine as a base required approximately 18 h to afford **2**, **3**, **4** and **5** in moderate yields; the only difference being in the latter where the product was precipitated by addition of water to its DMF solution. All of these pyrazine products were yellow or yellowish solids.

Using typical methods, cyclotramerisation reactions were carried out on these pyrazine derivatives to obtain the desired metal pyrazinoporphyrazines with the appropriate metal salt in different solvents such as DMF, quinoline, *n*-hexanol, 2-dimethylaminoethanol, *n*-pentanol as a high boiling solvent, in the presence of DBU as a catalyst. However from the range of solvents used only hexanol afforded products which were subsequently characterised as the hexyloxy pyrazinoporphyrazines. Although in some recent papers, it was reported that metal-free azapcs were prepared from pyrazine-dicarbonitrile derivatives with bulky

phenoxy substituents in quinoline at 160 °C, similar conversion of aryl- or arylalkyl-oxy-substituted pyrazine-dicarbonitriles **2–5** prepared during this work to Azapcs could not be realized either in the presence of metal ions or without any templating metal ion [22,23].

Changing the reaction conditions such as reaction temperature or solvents (e.g. DMF, 2-dimethylaminoethanol, etc.) did not lead to formation of any porphyrazines. A cyclotramerisation reaction occurred when *n*-hexanol and a hindered base 1,8-diazabicyclo[9.1.0]undec-7-ene (DBU) were used. However, this case transesterification took place in parallel in the basic medium and the products no longer carried the phenoxy-substituents but the hexyloxy-groups from the solvents instead. It should be considered as a reaction in line with the transesterification observed in the case of phthalocyanines with ester substituents [24]. Consequently, with the presence of DBU in *n*-hexanol **2**, **3**, **4** or **5** were reacted with zinc (II) acetate, cobalt and copper (II) chloride to form octakis(hexyloxy)pyrazinoporphyrazinato metal complexes **6**, **7** and **8**, respectively (Fig. 1).

Except for **6** (ca. 22% yield), compounds **7** and **8** were synthesized in relatively moderate yields in 36–52% range. These new octakis(hexyloxy)pyrazinoporphyrazinato metal complexes, **6**, **7** and **8** were purified by column chromatography on silica gel using methanol and chloroform as the eluent. They show high solubility in most organic solvents such as chloroform, dichloromethane, tetrahydrofuran, acetone and pyridine.

All new compounds were identified through several spectroscopic techniques including FT-IR, FAB-MS,  $^1\text{H}$  NMR, UV–Vis and elemental analysis. The spectroscopic data of the ligands were in accord with their assigned structures. Pyrazinoporphyrazines exhibited different vibrations from the substituent groups. Despite the pyrazine **2**, which did not have any aliphatic CH group in its structure, the stretching vibrations of aliphatic CH group for all the products **6**, **7** and **8** were observed as sharp and intense absorption bands appearing in 2956–2858  $\text{cm}^{-1}$ . The absorption band at around 3070  $\text{cm}^{-1}$  was characteristic for the aromatic CH group. This band disappeared upon conversion to **6**, **7** and **8** although all of these pyrazines contain an aromatic CH. In addition, the sharp peak at 2238  $\text{cm}^{-1}$  disappeared after conversion into the pyrazinoporphyrazines in support of the cyclotramerisation reaction of pyrazines. According to these results, IR spectral data of **6**, **7** and **8** indicate the formation of alkyloxy-pyrazinoporphyrazines.

In the case of zinc pyrazinoporphyrazine **6**,  $^1\text{H}$  NMR spectra indicated aliphatic  $\text{CH}_2$ ,  $\text{CH}_3$  and  $\text{O}-\text{CH}_2$  protons which are incongruous with the expected results. These data prove the presence of the unexpected hexyloxy pyrazinoporphyrazine. Furthermore, in the mass spectrum molecular ion peaks were noted at  $m/z$  1380.9 for **7** which confirmed incorporation of the hexyloxy unit.

Electronic absorption spectra of all pyrazinoporphyrazines **6**, **7** and **8** were analyzed in chloroform and all of them showed Q bands around 620 nm and B bands around 345 nm as expected for alkyloxy-substituted pyrazinoporphyrazines (Fig. 2) [25].

### 3.2. Voltammetric and spectroelectrochemical measurements

The solution redox properties of the complexes (**6–8**) were studied by using CV, DPV and DPSC techniques in DCM on a platinum electrode. Table 1 lists the assignments of the couples recorded and the estimated electrochemical parameters, which included the half-wave peak potentials ( $E_{1/2}$ ), and  $\Delta E_{1/2}$ . Table 1 also represents  $E_{1/2}$  values of related MPc and pyrazinoporphyrazine (PyPz) complexes in the literature for comparison [26–33]. The main difference of redox processes between the complexes **6–8** and the complexes reported in the literature are the peak potentials of the redox couples. All couples generally shifted approximately

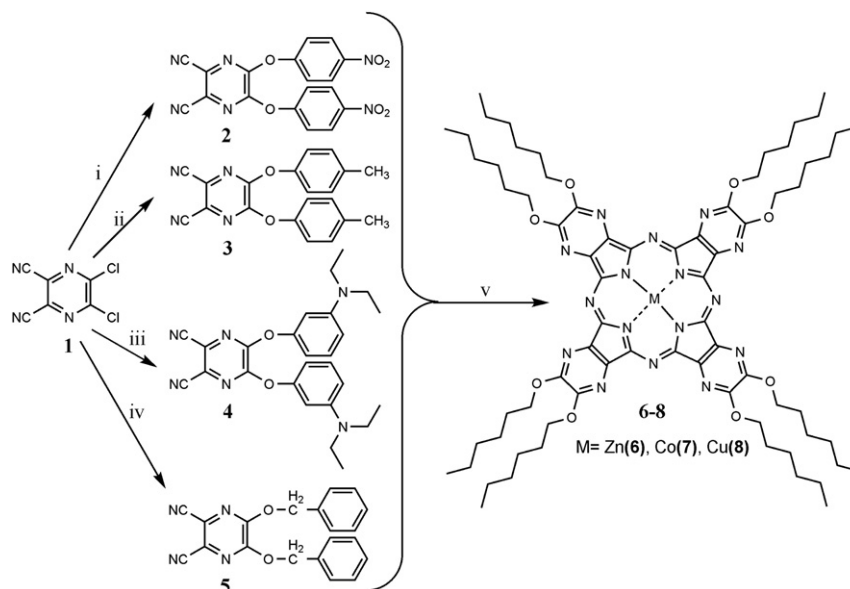


**Fig. 1.** Synthesis of Pyrazinoporphyrazines (i) *p*-nitrophenol, triethylamine, THF; (ii) *p*-cresol, triethylamine, THF; (iii) 3-(diethylamino)phenol, triethylamine, THF; (iv) benzyl alcohol, triethylamine, THF; (v) metal salts and/or DBU, Hexanol, 6 h, 135 °C.

0.20–0.40 mV towards positive potentials with respect to the MPCs having similar substituents [26–36]. These potential shifts of PyPz are due to the electron donating ability of the nitrogen atoms placed instead of carbons in the macrocyclic core of phthalocyanine analogues. Moreover, while the first oxidation process of CoPc complexes in a non-polar solvent is a ligand-based process, it is metal-based process for CoPyPz (7). As shown on the Table 1,  $DE_{1/2}$  values of MPyPz complexes studied here are slightly larger than that of the complexes reported in the literature. All complexes are aggregated in solution at high dilution. It is well documented that the introduction of nitrogen atoms to macrocyclic core can increase aggregation properties of the Pc complexes [37]. CV and DPV studies reveal that while CoPyPz (7) gives five well defined metal and/or ring-based redox couples, ZnPyPz (6) and CuPyPz (8) give only ring-based redox couples within the potential windows of the DCM/TBAP electrolyte and Pt electrode system.

Fig. 3 shows the CV and DPV of 7 in DCM containing TBAP. Complex 7 gave three one-electron reduction processes labelled as III at  $-0.05$  V (III' at  $-0.28$  V), IV at  $-1.13$  V, and V at  $-1.89$  V and two one-electron oxidation processes labelled as II at  $1.25$  V (II' at  $0.85$  V) and I at  $1.65$  V versus SCE at  $0.100$  Vs $^{-1}$  scan rate. The assignments of the redox couples are confirmed below using

spectroelectrochemistry measurements. As shown in Fig. 3, the first reduction and oxidation couples are split into two peaks. This behavior is due to the aggregation of the complex in solution. Dilution of the solution changes the aggregation–disaggregation equilibria of the complex (inset in Fig. 3A). When the solution is diluted the peak current of the wave III' assigned to the aggregated species became smaller than that of III, however it is present even in very diluted solution. The wave II' gives a small reverse couple during the reverse scan supporting the aggregation tendency of the complex.

Spectroelectrochemical measurements (SE) were used to confirm some of the assignments in the CVs. The experiments were performed using optically transparent thin-layer quartz electrochemical cell. Fig. 4A shows the in situ UV–vis spectral changes during the controlled potential reduction of 7 at  $-0.55$  V vs. SCE. There are two distinct changes during this potential application. First of all, while the intensity of the absorption of the Q band corresponding to the neutral  $[\text{Co}^{\text{II}}\text{PyPz}^{-2}]$  species decreases with a red shift from 606 to 612 nm, a new band corresponding to the electro-generated reduced  $[\text{Co}^{\text{I}}\text{PyPz}^{-2}]^{-1}$  species at 495 nm appears. Then while the intensity of the absorption of the Q band increases with red shift from 612 to 618 nm and the band at 495 nm increases in intensity, two new bands at 370 and 655 nm appear. At the same time the broadness of the Q band, due to aggregation, decreases during this potential application. The spectral changes in Fig. 4A are typical of metal-based reduction in porphyrin complexes. The shift of the Q band from 608 to 618 nm and the observation of new bands at 495 and 655 nm (MLCT) are characteristic of metal-based processes and assigned to  $[\text{Co}^{\text{II}}\text{PyPz}^{-2}]/[\text{Co}^{\text{I}}\text{PyPz}^{-2}]^{-1}$  [36,38–43]. The process at  $-0.55$  V potential application occurred with clear isosbestic points at 305, 366, 545, 611 and 681 nm in the spectra. The color of the solution changed from blue to red during the process. The reversion to the original spectrum after the potential application at 0.00 V indicates the reversibility of the process. During the controlled potential reduction of 7 at  $-1.30$  V vs. SCE corresponding to the redox process labelled IV (Fig. 4B), the absorptions for Q bands at 618 nm decreases in intensity without shift and the bands at 495 and 655 nm increase in intensity, while the band at 370 nm decreases in

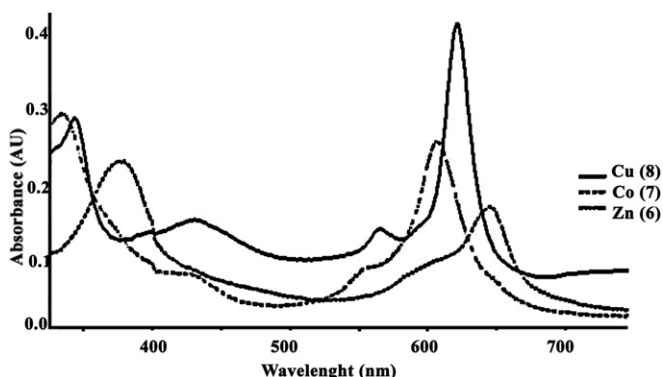


**Fig. 2.** UV–Vis spectra of compounds 6–8 ( $\text{CHCl}_3$ ,  $10^{-6}$  M).

**Table 1**  
Voltammetric data of the complexes with the related complexes from the literature for comparison.

Complex	Redox processes	Redox processes					$E_{1/2}$	Ref
		I	II <sup>b</sup>	III <sup>c</sup>	IV	V		
ZnPyPz (6) (V vs. SCE)	$E_{1/2}$	–	1.36 <sup>e</sup>	–0.53	–1.05	–1.73 <sup>e</sup>	1.89	tw
CoPyPz (7) (V vs. SCE)	$E_{1/2}$	1.65 <sup>e</sup>	0.85 (1.25) <sup>d</sup>	–0.05 (–0.28) <sup>d</sup>	–1.13	–1.88 <sup>e</sup>	0.90	tw
CuPyPz (8) (V vs. SCE)	$E_{1/2}$	1.50 <sup>e</sup>	0.97	–0.56	–1.10	–1.75 <sup>e</sup>	1.63	tw
<sup>g</sup> CoPc in THF	$E_{1/2}$ (SCE)	0.76	0.32	–0.21	–1.03	–1.25	0.53	26
<sup>h</sup> CuPc in DMSO	$E_{1/2}$ (SCE)	–	0.15	–0.95	–1.06	–1.90	1.10	27
<sup>i</sup> CoPc in DCM	$E_{1/2}$ (Fc <sup>+</sup> /Fc)	0.92	0.61	–0.29	–0.88	–1.38	0.90	28
<sup>i</sup> CuPc in DCM	$E_{1/2}$ (Fc <sup>+</sup> /Fc)	–	0.56	–0.91	–1.27	–	1.47	28
<sup>j</sup> ZnPc in DCM	$E_{1/2}$ (SCE)	–	0.85	–0.75	–1.16	–	1.60	29
<sup>k</sup> CoPc in DCM	$E_{1/2}$ (Ag/AgCl)	0.89	0.42	–0.40	–0.84	–	0.82	30
<sup>l</sup> ZnPc in DMF	$E_{1/2}$ (SCE)	1.16	0.48	–0.99	–	–	1.47	31
<sup>m</sup> ZnPyPz in DCM	$E_{1/2}$ (SCE)	1.03	0.65	–0.73	–0.94	–1.23	1.38	32
<sup>m</sup> CoPyPz in DCM	$E_{1/2}$ (SCE)	1.11	0.66	–0.24	–0.58	–0.97	0.89	33
<sup>n</sup> CuPyPz in DCM	$E_{1/2}$ (SCE)	–	–	–0.27	–0.66	–1.34	–	33

tw: this work.

<sup>a</sup>  $E_{1/2} = (E_{pa} + E_{pc})/2$  at  $100 \text{ mVs}^{-1}$  ( $E_{pc}$  for reduction,  $E_{pa}$  for oxidation for irreversible processes).

<sup>b</sup> This redox couple is a metal-based oxidation process for the complex 7.

<sup>c</sup> This redox couple is a metal-based reduction process for the complex 7.

<sup>d</sup>  $dE_p$  of the wave of aggregated species.

<sup>e</sup> Recorded by differential pulse voltammetry.

<sup>f</sup>  $\Delta E_{1/2} = \Delta E_{1/2}(\text{first oxidation}) - \Delta E_{1/2}(\text{first reduction}) = \text{HOMO-LUMO gap}$  for metal-free and metallophthalocyanines having electro-inactive metal center (metal to ligand (MLCT) or ligand to metal (LMCT) charge transfer transition gap for MPC having redox active metal center.

<sup>g</sup> Substituted with tetrakisdiethoxymalonyl groups.

<sup>h</sup> Substituted with propane 1,2-diolsulfanyl groups.

<sup>i</sup> Substituted with tetra(diethoxymalonyl) groups.

<sup>j</sup> Substituted with tetrapentafluorobenzoyloxy groups.

<sup>k</sup> Substituted tetrakis (benzylmercapto) groups.

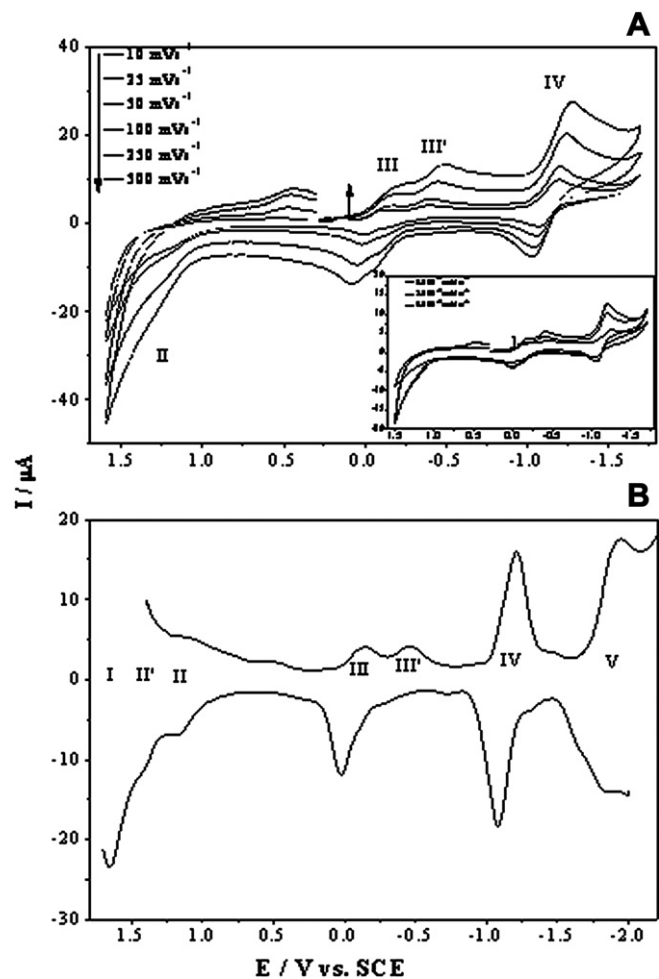
<sup>l</sup> Substituted tetra-(2-(2-thienyl)ethoxy) groups.

<sup>m</sup> Substituted with tetrakis-2,3-(5,7-diphenyl-1,4-diazepino) groups.

<sup>n</sup> Substituted with tetrakis-2,3-[5,6-di(2-pyridyl) pyrazino] groups.

intensity. The spectral changes in Fig. 4B are typical of ligand-based reduction assigned to  $[\text{Co}^{\text{II}}\text{PyPz}^{-2}]^{-1}/[\text{Co}^{\text{I}}\text{PyPz}^{-3}]^{-2}$  redox process [36,38–43]. The process at  $-1.30 \text{ V}$  vs. SCE potential application has isosbestic points at 330, 390, 549, 637 and 697 nm in the spectra. The color of the solution is changed from red to purple during the process.

On potential application at  $1.50 \text{ V}$ , the intensities of the Q bands increases with a red shift from 608 to 617 nm, while two new bands appear at 360 and 442 nm (Fig. 4C). At the same time while the B band shifts from 335 to 325 with a decrease in intensity, the broad Q band becomes sharp due to the disaggregation of the aggregated species during the process. The spectral changes in Fig. 4 C, especially shifting of the Q band with increasing intensity is typical of a metal-based oxidation in phthalocyanine and porphyrazine complexes and thus the process is easily assigned to  $[\text{Co}^{\text{II}}\text{PyPz}^{-2}]/[\text{Co}^{\text{III}}\text{PyPz}^{-2}]^{+1}$  redox process [38–43]. The process has isosbestic points at 313, 350, 376, 406, 510, 596, and 637 nm in the spectra and blue to green color changes upon the potential application at  $1.50 \text{ V}$ . Return to the original color and spectrum after the potential application at  $0.0 \text{ V}$  shows the reversibility of the process. It is well



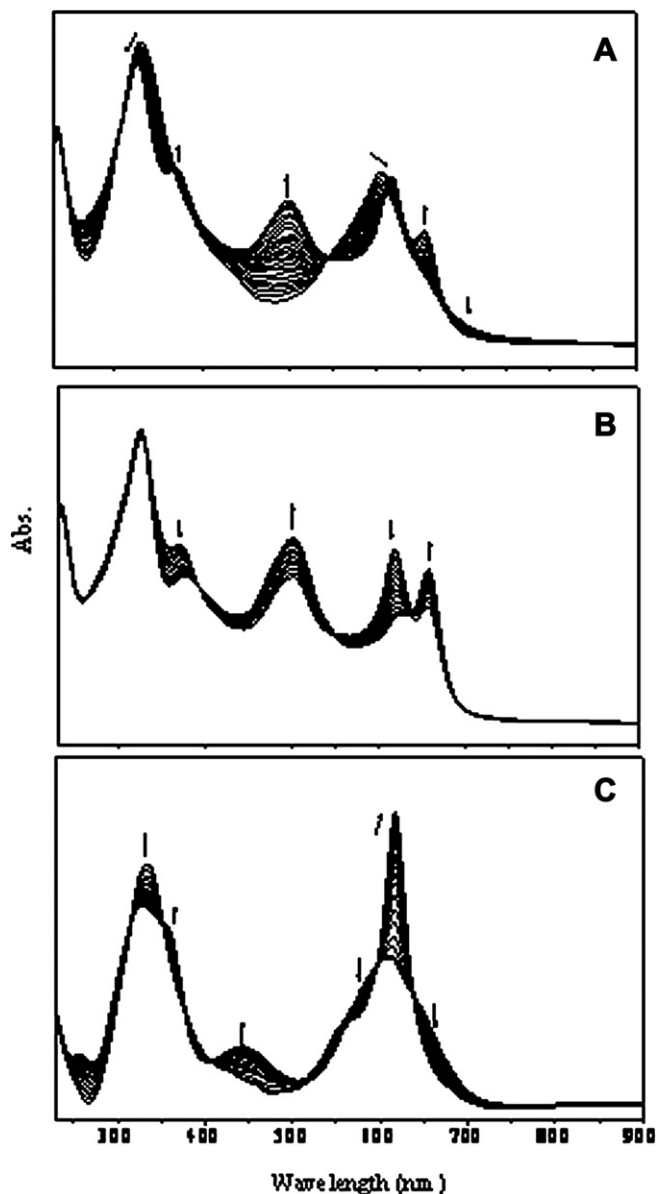


Fig. 4. In-situ UV-vis spectral changes of CoPyPz (7). A)  $E_{app} = -0.55$  V. B)  $E_{app} = -1.30$  V. C)  $E_{app} = 1.50$  V.

to the different metal center of the complexes (Table 1). Both complexes give three reduction redox couples and one oxidation process (two for **8**). Both complexes have a tendency to aggregate in solution even at very low concentration, a feature similar to complex 7. The values of  $I_{pa}/I_{pc}$ ,  $\Delta E_p$ , and  $I_p/v^{1/2}$  change with the concentration of the complex and the scan rate due to the aggregation–disaggregation equilibria present in solution [17,21]. As shown in Fig. 5, the redox couples of **6** are split into two peaks. This behavior is due to the aggregation of the complex in solution. Dilution of the solution changes the aggregation–disaggregation equilibria of the complex (inset in Fig. 5A). While the solution is diluted, peak current of the waves assigned to the aggregated species (II' and III') became much smaller than those of the waves corresponding to the monomeric species (II and III). Aggregation is also effective during the second reduction process (IV). At higher concentration, a new wave starts to appear just negative of the potential of the wave IV. Moreover, the process IV shifts to potentials that are more negative. DPV measurements (Fig. 5B) represent

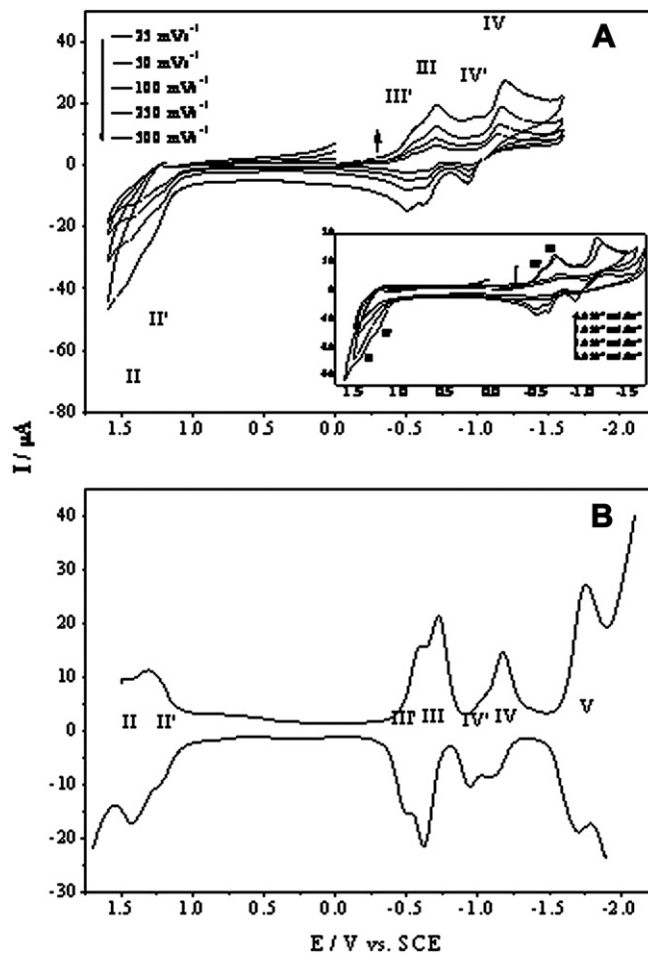
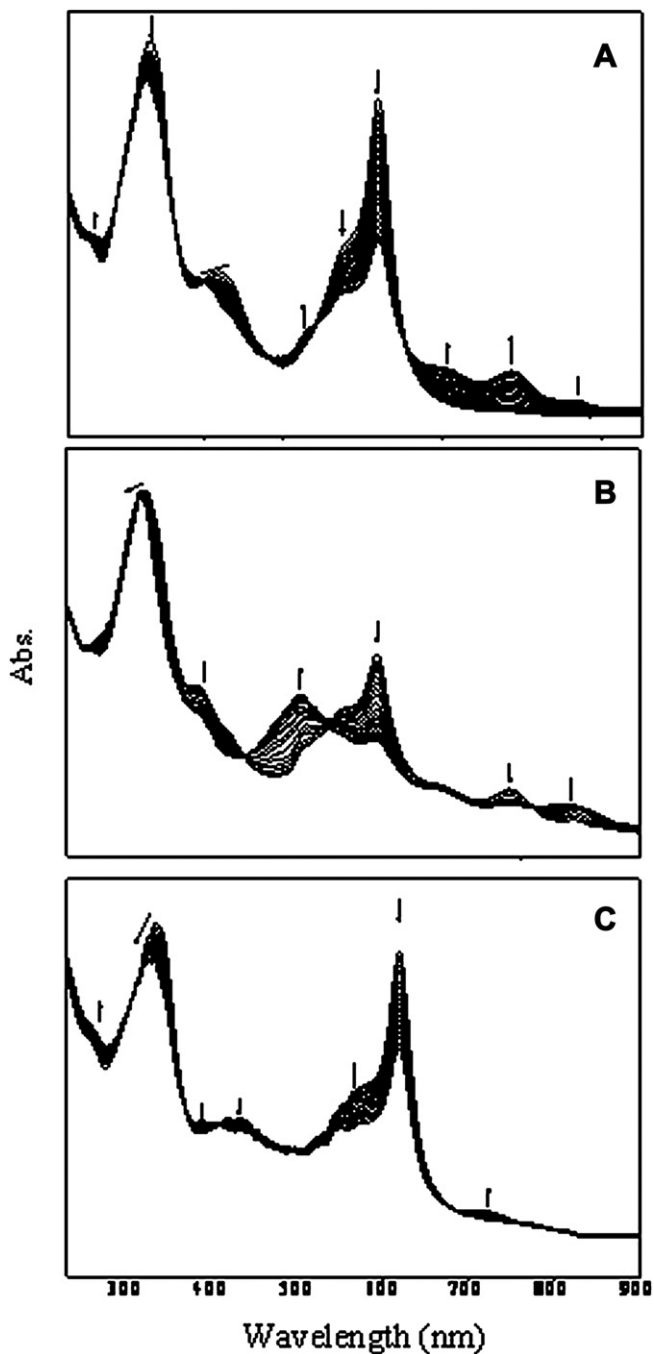


Fig. 5. A) CVs of ZnPyPz (**6**) ( $5.0 \times 10^{-4}$  mol dm $^{-3}$ ) at various scan rates on Pt in DCM/TBAP (Inset: CVs of ZnPyPz (**6**) at various concentrations at 0.100 Vs $^{-1}$  scan rate on Pt in DCM/TBAP). B) DPVs of ZnPyPz (**6**) ( $5.0 \times 10^{-4}$  mol dm $^{-3}$ ) (pulse time: 50 ms; pulse size: 100 mV, step size: 5 mV, sample period: 100 ms).

the splitting of the peaks due to the existence of aggregation–disaggregation equilibrium in solution.

The complexes **6** and **8** both have redox inactive metal centers. Therefore, in situ UV-vis spectral changes of **6** are given as a representative of the spectral changes of MPyPz having redox inactive metal center. Fig. 6 shows the in-situ UV-Vis spectral changes of **6** during the potential applications at the redox potentials. As shown in Fig. 6A, change of the intensity of the Q band at 618 nm without the wavelength shifting during the first reduction process of the complex and observation of new bands in the MLCT regions at 526, 706, 786 and 869 are characteristic of ring-based processes. During the process the Q band becomes sharper through decrease of the intensity of the shoulders of the Q band at 587 nm. At the same time, the B band at 393 nm decreases in intensity. The process has isobestic points at 294, 366, 400, 480, 540, and 654 nm in the spectra. Fig. 6B shows the spectral changes during the second ligand-based reduction of the complex under applied potential at  $-1.30$  V. Decrease in the intensity of Q band at 618 nm and observation of the new bands at 524 and 865 nm in the MLCT regions are characteristics of ring-based processes. Fig. 6C shows the ligand-based oxidation processes of the complex under the potential applications at 1.50 V. Decreasing of the intensity of Q band at 618 nm, and observation of the new bands at 390 and 720 nm in the MLCT regions are characteristics of ring-based processes [36–41].



**Fig. 6.** In-situ UV-vis spectral changes of ZnPyPz (6). A)  $E_{app} = -0.75$  V. B)  $E_{app} = -1.30$  V. C)  $E_{app} = 0.80$  V. B)  $E_{app} = 1.50$  V.

#### 4. Conclusion

In this work we have demonstrated the synthesis of four novel aryloxy and arylalkoxy-substituted pyrazines and their unexpected conversion to pyrazinoporphyrazines by replacement of the side groups with long chain alkoxides as a result of transesterification reaction in long chain alcohols such as hexanol. Voltammetric and spectroelectrochemical measurements present the well defined ring-based redox processes for zinc and copper and metal-based and/or ring-based redox processes for the cobalt analogue of pyrazinoporphyrazine in parallel with the relevant complexes. Redox processes were shifted to more positive

potentials due to the nitrogen atoms of the pyrazine parts of the complexes, which can be favorable for catalytic applications.

#### Acknowledgements

This work was supported by the Research Fund of the Technical University of Istanbul.

#### References

- [1] Jaung J-Y, Fukunishi K, Matsuoka M. Syntheses and spectral properties of 2,3,7,8 tetracyano-5,10-dihydrodipyrazino[2,3-b:2',3'-e]pyrazine. *Journal of Heterocyclic Chemistry* 1997;34(2):653–7.
- [2] Hou D, Matsuoka M. Reaction of 2,3-Dichloro-5,6-Dicyanopyrazine with amines. *Dyes and Pigments* 1993;22:57–68.
- [3] Morkved EH, Osletten H, Kjosens H. Preparation of Octa(alkoxy)azaphthalocyanines. *Acta Chemica Scandinavica* 1999;53:1117–21.
- [4] Morkved EH, Holmaas L, Kjosens H, Hvistendahl G. Preparation of Magnesium Azaphthalocyanines by cyclotetramerisation of 5-Substituted 4,5-Disulfanylpzazine-2,3-dicarbonitriles. *Acta Chemica Scandinavica* 1996;50:1153–6.
- [5] Suzuki T, Nagae Y, Mitsuhashi K. Synthesis of Pyrido[1',2':1,2]imidazo-[4,5-b] pyrazines from 2,3-Dichloro-5,6-Dicyanopyrazine with 2-Aminopyridines. *Journal of Heterocyclic Chemistry* 1986;23:1419–21.
- [6] Nakamura A, Ataka T, Segawa H, Takeuchi Y, Takematsu T. Structure-activity Relationships of Herbicidal 5-Ethylamino- and 5-Propylamino-2, 3-Dicyanopyrazines. *Agricultural and Biological Chemistry* 1983;47(7):1561–7.
- [7] Morkved EH, Kjosens H, Osletten H, Erchak N. Synthesis of Octa(dialkylamino) azaphthalocyanines. *Journal of Porphyrins and Phthalocyanines*. 1999;3 (6–7):417–23.
- [8] Hou D, Oshida A, Matsuoka M. Reaction of 2,3-Dichloro-5,6-Dicyanopyrazine with enamines and some tertiary amines. *Journal of Heterocyclic Chemistry* 1993;30:1571–5.
- [9] Stuzhin PA, Ercolani C. In: Kadish KM, Smith KM, Guillard R, editors. *Porphyrines with Annulated Heterocycles (97) in the porphyrin Handbook*, vol. 15. San Diego, California: Academic Press; 2003. p. 263.
- [10] Cristiano R, Westphal E, Bechtold IH, Bortoluzzi AJ, Gallardo H. Synthesis and optical/thermal properties of low molecular mass V-shaped materials based on 2,3-dicyanopyrazine. *Tetrahedron* 2007;63:2851–8.
- [11] Lee BH, Jaung JY, Jang SC, Yi SC. Synthesis and optical properties of push-pull type tetrapyrroloporphyrazines. *Dyes and Pigments* 2005;65:159–67.
- [12] (a) Moser FH, Thomas AL. *The phthalocyanines*, vols. 1 and 2. Boca Raton, FL: CRC Press; 1983; (b) Leznoff CC, Lever ABP. *Phthalocyanines: properties and applications*, vol. 1. New York: VCH; 1989. p. 5, 1992; vol. 2.
- [13] Reinert G, Holzle G, Graf G. GB Patent 2.159.516 A 1985; Reinert G, Holzle G, Graf G. *Chem Abstract*, 1986, 10: 25830.
- [14] Tanaka AA, Fierro C, Sherson DA, Yaenger E. Oxygen reduction on adsorbed iron tetrapyrroloporphyrazine. *Materials Chemistry and Physics* 1989;22 (3/4):431–56.
- [15] Yamana M, Kashawazaki N, Yamamoto M, Nakano T. A storage type electrochromic display utilizing Poly-Co-QTPP films. *Japanese Journal of Applied Physics Part 2* 1987;26(7):1113–5. L.
- [16] Murayama T, Macda S, Kurose Y. Japan Patent 61.291.187 1987; Murayama T, Macda S, Kurose, *Chem Abstract*, 1987, 107, 68274.
- [17] (a) Leznoff CC, Vigh S, Svirskaya PI, Greenberg S, Drew DM, Ben-Hur E. Synthesis and photocytotoxicity of some new substituted phthalocyanines. *Photochemistry and Photobiology* 1989;49(3):279–84; (b) Henderson BD. How does photodynamic therapy work? *Photochemistry and Photobiology* 1992;55(1):145–57.
- [18] Jaung JY. Characterization and optical properties of tetrapyrroloporphyrazines with phenylene dendron group. *Dyes and Pigments* 2007;75(2):420–5.
- [19] Fuchter MJ, Zhong C, Zong H, Hoffman BM, Barrett AGM. Porphyrines: designer macrocycles by peripheral substituent change. *Australian Journal of Chemistry* 2008;61:235–55.
- [20] Zimcik P, Miletin M, Kostka M, Schwarz J, Musil Z, Kopecky K. Synthesis and comparison of photodynamic activity of alkylheteroatom substituted azaphthalocyanines. *Journal of Photochemistry and Photobiology A: Chemistry* 2004;163(1–2):21–8.
- [21] Donald DS, Pont Du, U.S. Patent 3.879.394 1975; *Chemical Abstract*, 1975; 83, 133397.
- [22] Makhseed S, Samuel J, Ibrahim F. Synthesis and characterization of non-aggregating octa-substituted azaphthalocyanines bearing bulky phenoxy substituents. *Tetrahedron* 2008;64:8871–7.
- [23] Morkved EH, Andreassen T, Bruheim P. Zinc azaphthalocyanines with pyridin-3-yloxy peripheral substituents. *Polyhedron* 2009;28(13):2635–40.
- [24] Şener MK, Gül A, Koçak MB. Synthesis of tetra(tricarboethoxy)- and tetra(dicarboxy)- substituted soluble phthalocyanines. *Journal of Porphyrins and Phthalocyanines* 2003;7:617–22.
- [25] Stuzhin PA, Ercolani C. In: Kadish KM, Smith KM, Guillard R, editors. *Porphyrines with Annulated Heterocycles (101) in the porphyrin handbook*, vol. 15. San Diego, California: Academic Press; 2003. p. 331.

- [26] Koca A, Dinçer HA, Koçak MB, Gül A. Electrochemical characterization of Co(II) and Pd(II) phthalocyanines carrying diethoxymalonyl and carboxymethyl substituents. *Russian Journal of Electrochemistry* 2006;42(1):31–7.
- [27] Kandaz M, Çetin HS, Koca A, Özkaya AR. Metal ion sensing multi-functional differently octasubstituted ionophore chiral metallophthalocyanines: synthesis, characterization, spectroscopy, and electrochemistry. *Dyes and Pigments* 2007;74(2):298–305.
- [28] Şener MK, Koca A, Gül A, Koçak MB. Synthesis and electrochemical characterization of biphenyl-malonic ester substituted cobalt, copper, and palladium phthalocyanines. *Polyhedron* 2007;26(5):1070–6.
- [29] Koca A, Özkaya AR, Selçukoğlu M, Hamuryudan E. Electrochemical and spectroelectrochemical characterization of the phthalocyanines with pentafluorobenzoyloxy substituents. *Electrochimica Acta* 2007;52(7):2683–90.
- [30] Agboola B, Ozoemena KI, Nyokong T. Synthesis and electrochemical characterisation of benzylmercapto and dodecylmercapto tetra substituted cobalt, iron, and zinc phthalocyanines complexes. *Electrochimica Acta* 2006;51(21):4379–87.
- [31] Obirai J, Nyokong T. Synthesis, electrochemical and electrocatalytic behaviour of thiophene-appended cobalt, manganese and zinc phthalocyanine complexes. *Electrochimica Acta* 2005;50(27):5427–34.
- [32] Donzello MP, Dini D, D'Arcangelo G, Ercolani C, Zhan R, Ou Z, et al. Porphyrazines with annulated diazepine rings. 2. Alternative synthetic route to tetrakis-2,3-(5,7-diphenyl-1,4-diazepino)porphyrazines: new metal complexes, general physicochemical data, ultraviolet-visible linear and optical limiting behaviour and electrochemical and spectroelectrochemical properties. *Journal of the American Chemical Society* 2003;125:14190–204.
- [33] Donzello MP, Ou Z, Dini D, Meneghetti M, Ercolani C, Kadish KM. Tetra-2,3-pyrazinoporphyrazines with externally appended pyridine rings. 2. metal complexes of tetrakis-2,3-(5,6-di(2-pyridyl)pyrazino)porphyrazine. *Inorganic Chemistry* 2004;43(26):8637–48.
- [34] Lever ABP, Milaeva ER, Speier G. The redox chemistry of metallophthalocyanines. In: Leznoff CC, Lever ABP, editors. *Solution in phthalocyanines: properties and applications*, vol. 3. New York: VCH; 1993.
- [35] Lever ABP, Pickens SR, Minor PC, Licoccia S, Ramaswamy BS, Magnell K. Charge-transfer spectra of metallophthalocyanines: correlation with electrode potentials. *Journal of the American Chemical Society* 1981;103(23):6800–6.
- [36] Li R, Zhang X, Zhu IP, Ng DKP, Kobayashi N, Jiang J. Electron-donating or -withdrawing nature of substituents revealed by the electrochemistry of metal-free phthalocyanines. *Inorganic Chemistry* 2006;45(5):2327–34.
- [37] Kostka M, Zimcik P, Miletin M, Klemra P, Kopecky K, Musil Zbynek. Comparison of aggregation properties and photodynamic activity of phthalocyanines and azaphthalocyanines. *Journal of Photochemistry and Photobiology A: Chemistry* 2006;178(1):16–25.
- [38] Koca A, Özkaya AR, Arslanoğlu Y, Hamuryudan E. Electrochemistry, spectroelectrochemistry and electrochemical polymerization of titanylphthalocyanines. *Electrochimica Acta* 2007;52(9):3216–21.
- [39] Koca A, Dinçer HA, Çerlek H, Gül A, Koçak MB. Spectroelectrochemical characterization and controlled potential chronocoulometric demetallation of tetra- and octa-substituted lead phthalocyanines. *Electrochimica Acta* 2006;52(3):1199–205.
- [40] Matlaba P, Nyokong T. Synthesis, electrochemical and photochemical properties of unsymmetrically substituted zinc phthalocyanine complexes. *Polyhedron* 2002;21(24):2463–72.
- [41] Koca A, Özkaya AR, Selçukoğlu M, Hamuryudan E. Electrochemical and spectroelectrochemical characterization of the phthalocyanines with pentafluorobenzoyloxy substituents. *Electrochimica Acta* 2007;52(7):2683–90.
- [42] Hesse K, Schlettwein D. Spectroelectrochemical investigations on the reduction of thin films of hexadecafluorophthalocyaninatozinc (F<sub>16</sub>PcZn). *Journal of Electroanalytical Chemistry* 1999;476(2):148–58.
- [43] Donzello MP, Agostinetto R, Ivanova SS, Fujimori M, Suzuki Y, Yoshikawa H, et al. Tetrakis(thiadiazole)porphyrazines. 4. direct template synthesis, structure, general physicochemical behavior, and redox properties of Al(III), Ga(III), and In(III) complexes. *Inorganic Chemistry* 2005;44(23):8539–51.